Available online at www.sciencedirect.com
ScienceDirect
Journal of the European Ceramic Society 28 (2008) 1603–1612
www.elsevier.com/locate/jeurceramsoc

Nanostructured surface modification of microporous ceramics for efficient virus filtration

Markus Wegmann [a], Benjamin Michen [b], Thomas Graule [a,*]

[a] *Empa, Swiss Federal Laboratories for Materials Testing and Research, Laboratory for High Performance Ceramics, Überlandstrasse 129, CH-8600 Dübendorf, Switzerland*
[b] *Katadyn Products Inc., Birkenweg 4, CH-8304 Wallisellen, Switzerland*

Received 16 September 2007; accepted 2 November 2007
Available online 4 January 2008

Abstract

The aim of this study was to develop a depth filter working on the electrostatic adsorption principle based on a microporous diatomaceous earth water filter element. The internal surface area of the highly porous elements was coated with a colloidal nanodispersion of hydrated yttrium oxide and subsequently heat-treated under reducing conditions to yield filters featuring uniformly distributed electropositive Y_2O_3 coatings. Filters prepared in this fashion exhibit a flowrate of 60 l/h at 3 bar and remove in excess of 99.99% of 25 nm diameter MS2 bacteriophages from feed water between pH 5 and 9.

Keywords: Nanocomposites; Surfaces; SiO_2; Colloidal Y_2O_3; Membranes

1. Introduction

The removal of human pathogenic viruses from water poses a particular technological challenge because of the vanishingly small size of these particles (25–200 nm). Surface filtration (straining) methods such as nanofiltration and reverse osmosis, in which the liquid is forced through polymeric or ceramic membranes with pores smaller than the virus particles, are technically and commercially well-established and currently the only reliable means of removing viruses from drinking water.[b] However, next to fouling by other inorganic and organic materials suspended in the water such as dirt, bacteria and humic acids (HA) (a problem which affects all methods of filtration to some degree), two drawbacks are particularly characteristic of these surface filtration techniques: high cost and low flowrates.[1,2] With the world's growing populations putting increasing pressure on limited fresh water reserves and the risk of natural disasters and bio-terrorism ever-present, the need for virus filters with exactly the opposite characteristics, namely low cost with high flowrates at low pressure, is growing rapidly.[3]

A filtration technique with the potential to fulfill these two requirements is depth filtration by adsorption. The principle is that contaminated water is passed through a filter medium with micron-scale open porosity, and dispersed particles adsorb on the pore walls under the influence of van der Waals and electrostatic forces and hydrophobic interactions.[4] Because of the relatively coarse porosity (compared to the filtration membranes working on the straining principle described above), the flowrates should be high at low applied pressures, and the system cost should be greatly reduced because of the less demanding materials processing required and the absence of high-pressure pumps. The challenge is thus to develop a filter medium which will attract and trap virus particles at its surface and which possesses the largest possible adsorber area to provide the greatest possible capacity for adsorbed particles.

Various approaches have been presented in the literature which have taken up this challenge: diatomaceous earth (DE) modified with polyelectrolytes,[5–7] DE modified with salts/hydroxides of aluminum, iron, magnesium and calcium,[5,6,8] fiberglass and cellulose modified with salts of Al, Fe, Mg and Ca,[9] fiberglass and cellulose modified with alumina-coated colloidal silica,[10] sand modified with Fe- and

* Corresponding author. Tel.: +41 44 823 4123; fax: +41 44 823 4150.
E-mail address: thomas.graule@empa.ch (T. Graule).
[b] UV-disinfection is also a proven method with which to obtain virus-free water, however, it does not physically remove the virus particles from the water flow.

0955-2219/$ – see front matter © 2007 Elsevier Ltd. All rights reserved.
doi:10.1016/j.jeurceramsoc.2007.11.002

Al-hydroxide,[11] and granular anthracite and granular activated carbon coated with nanoporous Al_2O_3.[12] These and other studies of electropositive filter media[13,14] generally show that the strongest contribution to the adsorption process is made by electrostatic forces, i.e. the attraction of charged particles to an oppositely charged surface. Since water-borne viruses generally possess negatively charged surfaces (capsids),[4,15] the aim has been, and remains, the development of a highly porous filter medium which exhibits a positive surface charge (or zeta potential[16]) over the widest possible pH range.

As several research groups had done in the past,[5–8] the authors selected to use diatomaceous earth ceramic (DE; also known as kieselguhr, a highly porous form of naturally occurring SiO_2) as the base material for a high-flowrate virus-adsorbing filter.[17,18] Since this abundantly available silica-based filter medium, exhibiting an isoelectric point (IEP) around pH 2 is therefore generally negatively charged when immersed in water, the authors applied a nanostructured, high-specific surface area coating of zirconia to the internal surface area of extruded DE filter elements in an effort to impart a high adsorption capacity and generally positively charged surface to the filter. While promising microbiological results when filtering MS2 bacteriophages[c] were obtained, the applied coatings either failed to adsorb virus particles across the entire desired pH range (5–9), or were washed out by the passage of water through the filters.

The results from this study were promising enough to warrant further pursuit of the development approach, albeit with an alternative coating material. Applying the theory of Parks[22] and atomic radius data tabulated by Shannon,[23] yttrium oxide (Y_2O_3) was pinpointed as a potential adsorber with an IEP in the range 9.3–9.7, i.e. the material is positively charged in water at lower pH values, and negatively charged at higher pH values. The IEP range of 7.4–10.2 determined in the course of a detailed literature review on the subject of real measurements on aqueous Y_2O_3 dispersions by Kosmulski[24] is considerably wider, but the average of pH 8.8 agrees well with the theoretical expectation and Y_2O_3 was consequently selected as the coating material with which to continue the development of a practical high-flowrate virus filter. In order to be suitable for practical applications, the finished filter must exhibit a flowrate of 60 l/h at an operating pressure under 3 bar. Furthermore, as a prerequisite to being certified as a true virus filter by the United States Environmental Protection Agency (USEPA), the unit must remove in excess of 99.99% of viruses from feed water containing 10^7 plaque forming units (PFU) per liter between pH 5 and 9.

2. Experimental

2.1. Materials

As in the previous study by the authors involving zirconia coatings,[17] the filter element type used for this work was the diatomaceous earth-based "Pocket" element manufactured by Katadyn Products Inc. The tubular filters are produced by aqueous extrusion of a proprietary mixture of diatomaceous earths, layered silicates and organic binders followed by drying and gas firing at temperatures in excess of 1000 °C. The characteristics of this filter medium are summarized in Table 1, and a representative micrograph of its highly microporous microstructure is shown in Fig. 1.

Table 1
Characteristics of the basic tubular filter element of type "Pocket"

Filter type	Depth
Mean pore size (μm)[a]	0.2–2
Specific surface area (m^2/g)[b]	2.2
Geometrical density (g/cm^3)	0.85
Length (cm)	12.15
Outer diameter (cm)	4.0
Inner diameter (cm)	2.55
Throughput (l/h)[c]	60
0.5–2 μm bacteria reduction (%)[d]	99.9999

[a] Mercury intrusion porosimetry.
[b] BET.
[c] Deionized water at 3 bar and 25 °C.
[d] *Klebsiella terrigena* (ATCC333-257)[25] and *Pseudomonas aeruginosa*.[26]

The material chosen with which to coat the filters was NYACOL® colloidal yttria (Nyacol Nano Technologies Inc., USA), an aqueous acetate-stabilized suspension of positively charged 10 nm particles at pH 7 (manufacturer's specification). Simultaneous laser non-invasive back scattering and electrophoresis measurements yielded an average particle size of 3.5 nm and a positive surface charge of 13 mV at pH 7 (Zetasizer Nano ZS, Malvern Instruments, UK). While the product name (yttria) indicates a crystalline material, X-ray analysis showed that the particles are initially amorphous and that heat treatments are required to promote development of the crystalline phase (Fig. 2). As the physico-chemical nature of the nanoparticles in the colloid is thus unclear, the material is referred to in the remainder of the text as either "$Y(OH)_x$" or hydrated yttrium oxide. The Y_2O_3 yield of the colloid after drying and subsequent calcining at 1000 °C in air was 14 wt.%, which correlates exactly with the manufacturer's specifications.

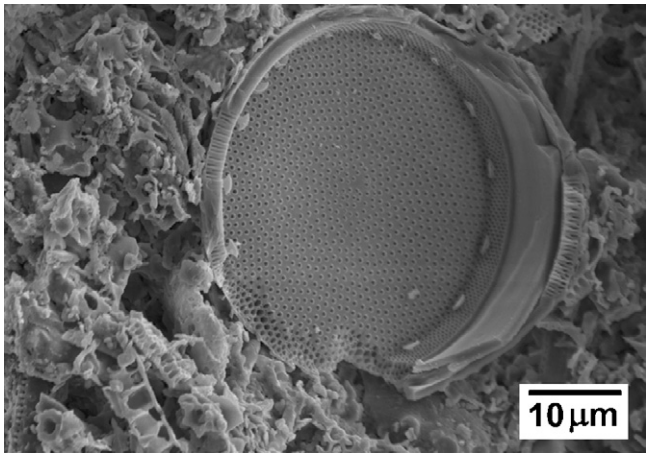

Fig. 1. SEM micrograph of the microstructure of a DE-based filter element as used in this study (fracture surface).

[c] The MS2 coliphage is a single-strand RNA bacteriophage 24–26 nm in diameter.[19] With an IEP of 3.9,[20] MS2 has established itself as a reliable nonpathogenic virus-like challenge particle for filter tests.[14,21]

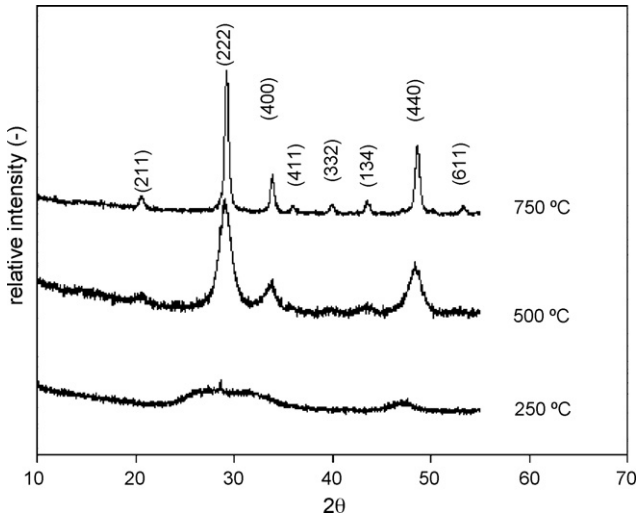

Fig. 2. XRD patterns of the $Y(OH)_x$ colloid dried 12 h at 80 °C and calcined 1 h under air at the specified temperatures. Significant crystallinity was already obtained at the relatively low temperature of 500 °C.

The electrophoretic method was used to determine the zeta potentials of the calcined colloid powders across a range of pH values (Zetasizer Nano ZS, Malvern Instruments, UK). The powders were ball-milled 18 h in PE bottles in ultra-high purity water ($R = 18\,M\Omega$, TOC<20 ppb, residual particle size <50 nm) with 5 mm ZrO_2 balls. Immediately prior to measurement this dispersion was diluted to a concentration of ≈0.001 wt.% with the same ultra-high purity water adjusted to a conductivity of 400 μS/cm with NaCl (ACS reagent, Sigma–Aldrich). In order to obtain the pH-dependency of the zeta potential, either 0.1 M HCl or 0.1 M NaOH (ACS reagents, Sigma–Aldrich) were added to the dispersion.

2.2. Filter modification

The highly porous filter elements were dip-coated in the hydrated yttrium oxide colloid for 2 h at ambient pressure. Capillary forces alone were responsible for drawing the colloid into the filter structure. Calculations based on the porosity of the filter medium, the density of the colloid, and the weight-gain measured immediately after removal of the elements from the coating bath showed that ≈90% of the pore volume was filled during this step. After dip-coating the filter elements were dried in air for 12 h at 80 °C in a laboratory-drying oven. Problems with and modifications to this basic dip-coating process are described below in Section 3.

After coating and drying the elements were heat-treated (calcined) 1 h in an electric tube furnace (HST 15/610 1500 °C Split Tube Furnace, Carbolite Furnaces Ltd., UK) at temperatures between 500 and 1040 °C under either static air, or a mixture of 92% N_2/8% H_2 flowing at 0.5 l/min to consolidate the coating and obtain the desired Y_2O_3 phase.

2.3. Physical and chemical characterization

Microstructural analyses were performed using scanning electron microscopy (SEM; JSM-6300F, JEOL Corp., Japan/Vega TS 5130, TeScan s.r.o., Czech Republic). The JSM-6300F was equipped for energy dispersive spectroscopy (EDS), thereby enabling standardless semi-quantitative elemental analyses of the microstructures. Samples were mounted on Al sample stubs using either carbon paste or carbon tape, and sputter coated with either Au–Pd or C. Analyses were generally performed at working distances of 15–20 mm with a 20 kV acceleration potential.

Phase analyses were obtained using powder X-ray diffraction (XRD; X'Pert Pro MPD, PANalytical B.V., The Netherlands). Samples were crushed to fine powders with an agate mortar and pestle and sprinkled on single-crystal Si stubs covered with a thin layer of vaseline. Measurements were performed with Cu Kα radiation (40 mA filament current, 40 kV accelerating potential) in steps of 0.017° 2θ.

The specific surface areas of selected filter samples were determined by the Brunauer–Emmet–Teller (BET) method (Model SA3100, Beckman-Coulter, USA). The specimens were cut into roughly 2 mm × 2 mm × 2 mm pieces with a diamond wheel and dried/degassed under flowing nitrogen at 200 °C for 3 h before the measurements were conducted.

Elemental analyses of eluates obtained from filter performance tests (see below) were performed using inductively coupled plasma emission spectroscopy (ICP) by an external contract laboratory (SGS Institut Fresenius GmbH, Taunusstein, Germany).

2.4. Filter performance

The streaming potential method was applied to quantify the effect of the coatings on the zeta potential of the filter medium. First, wafers of the virgin filter ceramic 14 mm in diameter and 1 mm thick were coated with $Y(OH)_x$ and heat-treated as outlined above. A wafer would then be mounted in an electrokinetic analyzer (SurPASS, Anton Paar GmbH, Austria) and rinsed with background electrolyte, a 10^{-3} M solution of KCl (p.a. grade KCl, Carl Roth GmbH, in ultra-high purity water) prior to the first measurement. Additions of 0.1 M NaOH (standard solution, Carl Roth GmbH) to the electrolyte solution permitted the pH-dependence of the streaming potential to be determined in the range pH 6–10. The obtained streaming potential data was subsequently mathematically treated according to the method of Fairbrother and Mastin[27] to yield the desired zeta potential series. Since the wafers were measured in the so-called "flow-through" mode where the electrolyte is forced to flow through the wafer rather than simply pass it ("cross-flow"), these measurements model the filter application in miniature and yield zeta potential information for the internal pore structure of the filter medium.

Visual screening retention tests were performed with microbiologically inert fluorescent monosized latex microspheres (Fluoresbrite® YG carboxylate microspheres 0.05 μm, Polysciences Inc., USA). These carboxylate-modified microspheres have a negative zeta potential and a particle size of 39.3 ± 5.0 nm across the pH range 3–9, characteristics which make them ideal model particles to represent well dispersed, non-coagulated viruses.[17] A bright-yellow dispersion with

≈10^{15} monospheres/L in a standardized water (see below) was manually pumped through the filter under test (20 °C/pressure cycles ≈0–10 bar) and any obvious reduction in the coloration of the eluate relative to the feed dispersion was noted.

MS2 coliphages were used to determine the retention performance of the filters prepared in this study. The host bacterium *Escherichia coli* (DSM 5695) and the MS2 phages (DSM 13767) were obtained from the German Collection of Microorganisms and Cell Cultures (DSMZ, Germany). Following reactivation and propagation of the MS2 phages, feed suspensions with a phage concentration of approx. 10^7 PFU per liter of water were prepared and assayed by the single-agar-layer (SAL) method.[d,28] After shifting the pH of the feed suspensions to the desired value using 0.1 M NaOH and/or 0.1 M HCl (ACS reagent, Sigma–Aldrich), these were pumped through a given filter (25 °C/3 bar) and the SAL assay repeated with the collected eluate. Comparison with the feed assay yielded the retention performance in terms of the log removal value (LRV = −log(1 − Ri), where Ri is the fractional retention). The SAL assay was also repeated during the duration of a test with the unfiltered pH-shifted feeds to check for fluctuations/reductions in the phage concentration over time. No significant phage concentration changes in the feed suspensions over time, or due to a pH-shift, were recorded in the course of the study.

Two types of water were used to conduct the latex and MS2 retention tests, namely potable tap water as supplied from the domestic mains, and a "standardized" water as defined in the previous study by the authors.[17] This consisted of deionized water with an initial pH of 5 and a base conductivity of 20 μS/cm in which NaCl (ACS reagent, Sigma–Aldrich)[e] was dissolved to adjust the conductivity to 400 μS/cm.

3. Results and discussion

3.1. Zeta potentials

The results of the electrophoretic measurements are shown in Fig. 3. The shaded band between pH 5 and 9 represents the range in which the USEPA requires that a virus filter must remove viruses.[25] Therefore, in the case of an adsorption filter, its surface should exhibit a positive surface charge across this range to effectively attract negatively charged viruses (represented here by MS2 bacteriophages). Under oxidizing conditions, calcining the dried $Y(OH)_x$ colloid yields a powder with an IEP of 8.2 (1 h at 550 °C in air). The switch to a negative surface potential above this pH means that the coating material in this form would repel/desorb viruses above pH 8.2 and therefore would fail as an effective adsorber below the stipulated upper threshold.

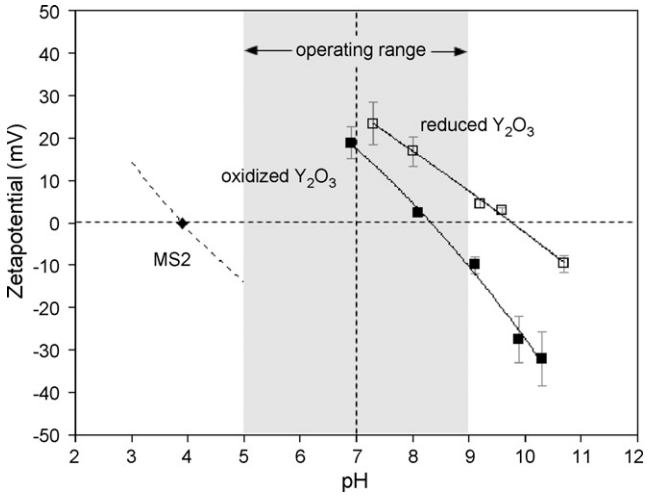

Fig. 3. Zeta potentials as obtained by electrophoretic measurements of $Y(OH)_x$ powder after calcining 1 h at 550 °C either under air (oxidized), or under flowing 92% N_2/8% H_2 (reduced). The literature value of the IEP of MS2 bacteriophages at pH 3.9[20] and their idealized pH-dependence are shown for reference.

As expected from the literature,[22] calcining under a reducing atmosphere (92% N_2/8% H_2) shifts the IEP of the Y_2O_3 particles further into the basic regime to pH 9.8. This can be understood by considering that under the reducing atmosphere, O^{2-} ions are removed from the surface of the powder particles, resulting in a net positive imbalance of the surface charge. The shift of the IEP above pH 9 makes this material very interesting for use in a virus adsorption filter because it can potentially meet the USEPA requirement.

The results of the streaming potential measurements of coated filter material are shown in Fig. 4. The considerable shift in the zeta potential of the coated medium relative to the uncoated

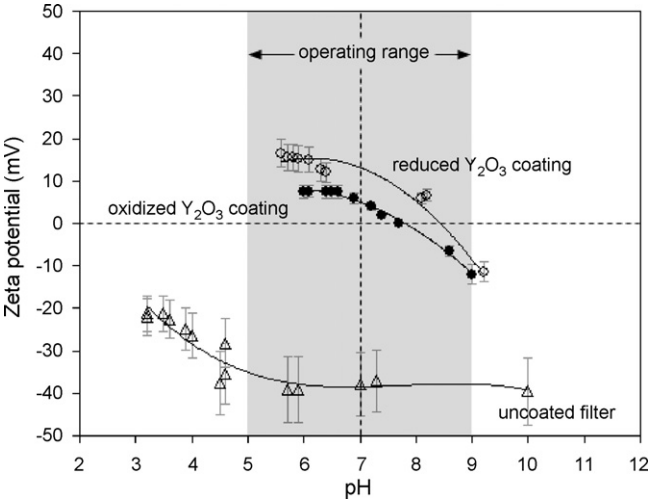

Fig. 4. Zeta potentials as measured by the streaming potential method of the base filter medium and of filter medium coated with undiluted $Y(OH)_x$ and calcined 1 h at 500 °C under either oxidizing or reducing conditions. The samples were 1 mm thick and were measured in the flow-through mode which models the filter in operation in miniature.

[d] A 100 ml sample (or 100 ml dilution thereof), 5 ml calcium chloride solution and 5 ml host bacterium exponential culture are mixed with SAL agar at 44.5 °C. This mixture is evenly distributed over 12 petri dishes and solidified at room temperature for 30 min. The plaque forming units are counted after inverting the plates and incubating them at 37 °C for 16–20 h.

[e] NaCl was chosen in order to keep the ionic strength low, i.e. to prevent excessive compression of the electrical double layer. By preventing particle coagulation, this ensured that sieving of large multiparticle agglomerates in the filters could be discounted.

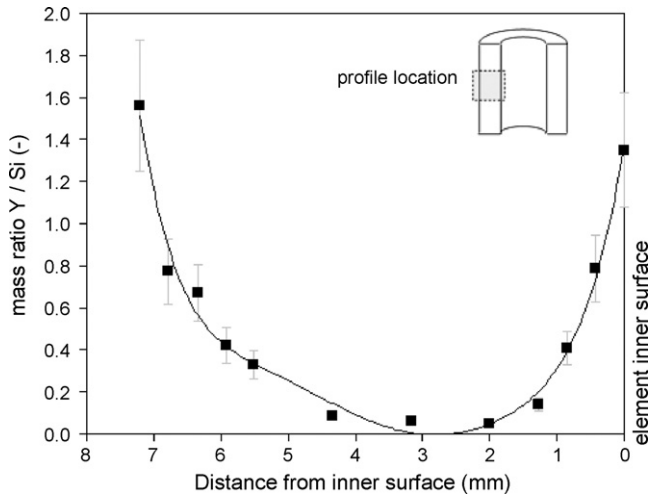

Fig. 5. Yttrium profile as measured by SEM/EDS through the wall (inset) of a filter element coated with the as-delivered $Y(OH)_x$ colloid according to the basic procedure described in Section 2 (air-dried at 80 °C for 12 h with the tube ends open, calcined at 500 °C for 1 h under static air).

material indicates that the Y_2O_3 coating effectively screens the diatomaceous earth ceramic from the flowing electrolyte. In this case, the application of the reducing atmosphere causes an increase in the measured IEP from pH 7.7 to 8.5. The fact that this range is shifted approx. 1 pH unit to the left compared to the electrophoretic data in Fig. 3 can be understood by considering that the Y_2O_3 particles most likely do not form a flawless coating on the base filter medium. As a result, a finite area of the underlying DE-based material ($IEP_{SiO_2} \approx 2.8$)[25] will be in contact with the electrolyte and thereby contribute an acidic component to the measured zeta potential, shifting the IEP towards lower pH values.

3.2. Coating distribution

In the previous study performed with a $Zr(OH)_x$ colloid, it was observed that the nanometric colloid particles migrated towards the inner and outer surfaces of the tube-shaped DE-based filter elements during drying, resulting in a U-shaped concentration profile of the coating material across the tube wall.[17] This behavior was also observed in the current work, as shown in Fig. 5. Since this phenomenon leads to blockage of porosity in the near-surface regions of the filter and thereby reduces the flowrate possible at a given operating pressure, various approaches were considered in the current study to flatten the concentration profile as far as possible.

Immobilizing the nanoparticles by gelling the colloid was investigated in some detail. Since the filter element had to be infiltrated completely with the fluid colloid before the gelation event could be allowed to occur, a degree of experimental control over the gelation onset had to be available. This control was available through the colloid temperature in the case of gelation with additions of agarose (thermal gelling upon cooling) and in the case of gelation induced by a time-delayed pH-shift with additions of urea and urease (principle of direct coagulation casting, or DCC[29]).

For the former trials, agarose (Type IX ultra-low gelling, Sigma–Aldrich) was dissolved in the colloid at 80 °C while the filter element was likewise preheated dry to 80 °C. The agarose concentration was varied between 0.2 and 2 wt.% with respect to the water content of the colloid. Infiltration was performed as usual for 2 h, but with the system temperature held at 80 °C. After infiltration the element was refrigerated at 5 °C for several hours, gelation of the colloid occurring upon cooling below approx. 50 °C. Drying was conducted for 12 h in air at 40 °C, which was confirmed to be 10 °C under the remelting temperature of the gel ($T_{remelt} \approx 50$ °C). The elements were calcined at 500 °C for 1 h.

Surprisingly, despite the pronounced gelling effect observed upon cooling the colloids containing agarose, the yttrium profiles showed little improvement relative to those obtained using the basic procedure (Fig. 6; compare with Fig. 5). It appears that although the agarose molecules form a gel, the network porosity is large enough to permit the passage of the colloid particles and that their migration with the carrier water is not prevented. As the desired effect could not be achieved, this gelation route was not pursued further.

For the DCC experiments, urea (purum, ≥99.0%, Fluka) was dissolved in the colloid (9 wt.% urea with respect to colloid water content) at room temperature in preparation for the infiltration step. Urease (powder Type IX, Sigma–Aldrich) was dissolved in deionized water (0.1–1 wt.% with respect to urea) and added to the colloid immediately prior to immersing the filter element. As described in detail in Ref. [29],[29] the urease catalyzes the hydrolysis of the urea, releasing ammonia molecules into the system and shifting the pH to higher values, thereby destabilizing the colloid and causing a gel to form through particle–particle coagulation. This is a slow process, with a gelation effect only becoming apparent after approx. 45 min with the 1 wt.% urease addition. Reducing the urease concentration to 0.1 wt.%

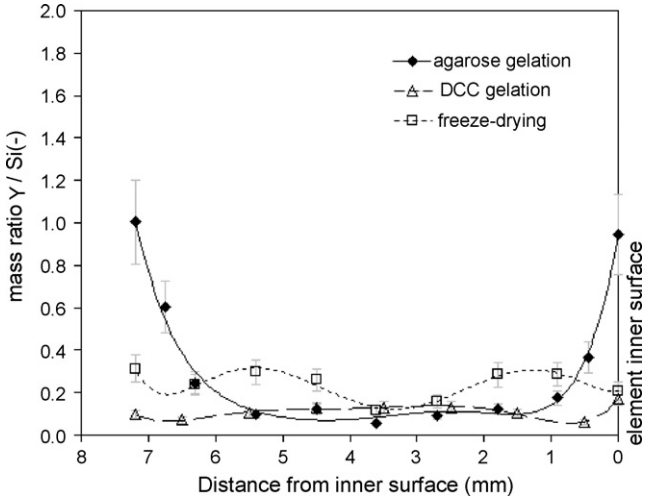

Fig. 6. Yttrium profiles as measured by SEM/EDS through the walls of filter elements coated using three modifications of the basic $Y(OH)_x$ coating procedure: (1) colloid gelation with 0.8 wt.% agarose addition; (2) direct coagulation casting (DCC) with urea/urease addition; (3) freeze-drying. All elements were subsequently air-dried at 80 °C for 12 h with the tube ends open and calcined at 500 °C for 1 h under static air.

increased the gelation onset delay to approx. 90 min. After 2 h total residence time, the filter elements were removed from the gelled colloid, wiped clean of excess gel, dried 12 h in air at 80 °C, and calcined 1 h at 500 °C.

As shown by the flat compositional profile of yttrium through the filter wall in Fig. 6, gel formation in this case successfully prevented colloid particle migration during drying. However, measurements of the specific surface areas of these coated filters yielded values around 2 m^2/g, representing absolutely no improvement over the virgin DE filter (2.2 m^2/g, Table 1). Thermal–mechanical and SEM analysis of the gelled colloid revealed a sharp sintering onset at only 200 °C and extremely rapid sintering, which caused the nanoporous microstructure of the coating to be lost in a matter of minutes.[f] It may be speculated that shifting the colloid pH and bringing the colloid particles into close contact with one another (presumably into the primary attractive minimum of the force vs. separation curve[16]) enables a solid-state diffusional exchange between the particles which favors a rapid reduction of the high surface-free energy of the nanoparticle gel network. As noted in the introduction, a prerequisite for a successful virus adsorption filter is a high internal surface area, and because this could not be achieved when applying the DCC process, the method was neither developed nor analyzed any further in this study.

Another approach considered to prevent particle migration after infiltration was freeze-drying. The colloid-saturated filter elements were frozen 12 h at −5 °C, dipped into liquid nitrogen (−196 °C) for 5 min, and immediately placed under a 5×10^{-2} mbar vacuum in a glass bell jar. The vacuum was held for approx. 4 h, at which point the filter elements were removed from the bell jar and refrozen in liquid nitrogen for 5 min while the liquid nitrogen-cooled cold trap in the vacuum line was thawed to remove the frozen water condensate. This procedure was repeated four times over a period of 2 days. Final drying was performed for 12 h in air at 80 °C, and heat-treatment was performed 1 h at 500 °C.

This procedure yielded fairly flat yttrium profiles across the filter wall, as shown in Fig. 6, and acceptable specific surface areas were achieved (15 m^2/g). Because the water is sublimated into the gas phase from the frozen state, no fluid flow occurs during drying and particle migration is prevented. Theoretically particle migration should be completely prevented, but the data suggest that some migration occurred. Because the filter elements were only frozen in liquid nitrogen prior to applying the vacuum and were not actually cooled during the drying process, it is likely that despite the thermal insulation provided by the vacuum, the filter elements slowly warmed up during the process and that some thawing of the colloid occurred before the elements were refrozen. Despite these promising results, the procedural complexity and the associated limited throughput of the process precluded it from being used as the standard infiltration procedure in this study.

[f] After being calcined 1 h at 500 °C, the dried colloid without any additions of urea and urease exhibited a specific surface area of 150 m^2/g and filter elements coated by the basic infiltration process 16 m^2/g.

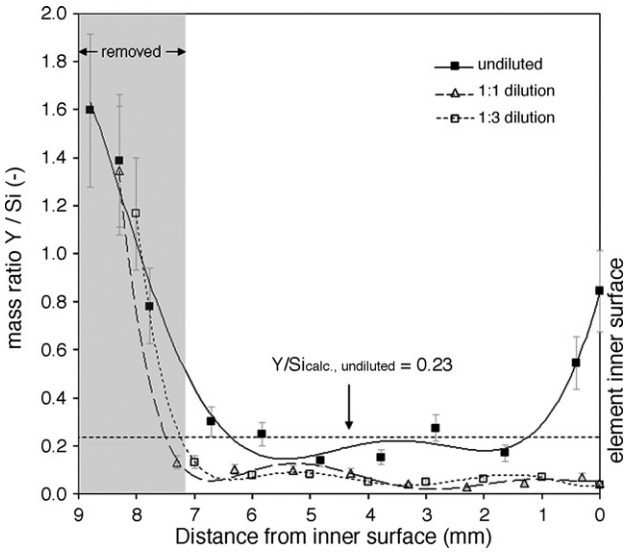

Fig. 7. Yttrium profiles as measured by SEM/EDS through the walls of over-dimensioned filter elements coated with three different concentrations of $Y(OH)_x$ colloid (air-dried at 80 °C for 12 h with the tube ends closed off, calcined at 500 °C for 1 h under static air). The shaded region represents that material which is mechanically removed by turning to yield the finished filter element with a required wall thickness of 7.25 mm. The horizontal reference lines show the Y/Si ratio expected from calculations based on the weight-gain, measured porosity and the particle loading in the undiluted colloid.

The solution ultimately chosen was the following: Instead of infiltrating filter elements with standard dimensions as previously (refer to Table 1), elements with a slightly larger outer diameter were used. During drying, the ends of the filter tubes were capped with pieces of snug-fitting rubber sheet to prevent drying from the inner surfaces, thereby forcing water diffusion and particle migration to occur primarily towards the outer surface. This resulted in the skewed U-shaped yttrium concentration profile shown in Fig. 7, which is weighted towards the outer surface. By subsequently machining the outer diameter of the filter tube down to the standard dimension, elements were produced which exhibited a largely uniform coating concentration across the tube wall.

Consideration of the filter medium area to be coated (≈2.2 m^2/g) and the concentration of $Y(OH)_x$ particles in the as-delivered colloid indicates that enough colloid particles are introduced into a given filter element during the infiltration step to coat the available DE area several times over. This, in turn, further explains the observed gradient formation during drying: As noted in Section 2 above, the colloid particles possess a positive surface charge at pH 7, and as shown in Fig. 4, the base filter possesses a negative surface charge at this pH. Therefore, during infiltration of the colloid into the filter medium, the first (few) layer(s) of nanoparticles will be strongly adsorbed by virtue of the opposing charges on the particles and the substrate. This initial adsorption neutralizes the net negative charge at the filter surface and greatly weakens the tendency for further adsorption of nanoparticles to the coating. Thus, while sufficient particles are present to coat the filter medium several layers thick, there is no force to promote coating growth past the first few layers, and the excess particles are subsequently swept towards the filter surface by capillary forces during the drying process.

A reduction in the particle concentration in the colloid should therefore reduce the tendency for the gradient to form during drying. This was confirmed when infiltration was performed with the colloid diluted 1:1 (by volume) and 1:3 with ultra-high purity water, as shown in Fig. 7.

3.3. Flowrate and filter surface area

Next to the reducing the concentration gradient and the amount of expensive colloid lost during the final machining step, another beneficial effect brought about by diluting the $Y(OH)_x$ colloid was an increase in the flowrate through a filter element at a given pressure. While filters coated using the as-delivered colloid and calcined at 550 °C achieved an average of 45 l/h at 3 bar operating pressure, equivalent filters prepared with the 1:1 dilution averaged 60 l/h. This result is expected because less coating material in the filter equates to more open pore volume and hence a larger open cross-section through which water can flow.[g]

A penalty incurred by diluting the colloid was a reduction in the achievable specific surface area (SSA): after calcination at 550 °C, for example, the element modified using the as-delivered colloid exhibited a SSA of 13.5 m^2/g, while the element dip-coated in the 1:1 dilution exhibited only 8 m^2/g (compared with 2.2 m^2/g for the basic DE element). Logically, by decreasing the number of nanoparticles in the microstructure, the contribution of the high SSA-coating to the total area in the filter is reduced. Such a reduction should be minimized, since the filter capacity of a filter functioning by the principle of adsorption is directly proportional to the available internal surface area.

Here it should be noted that the specific surface area is also strongly influenced by the calcining temperature, as shown in Fig. 8. As expected, as the heat-treatment temperature increases, the specific surface area decreases because sintering processes cause significant growth of the nanoparticles: BET measurements of the dried and calcined colloid itself yielded a SSA of 150 m^2/g after treatment at 500 °C and 0.7 m^2/g after treatment at 1040 °C, which corresponds to average primary particle sizes of 8 nm and 1.7 μm, respectively. As mentioned above, it is undesirable to reduce the surface area too much as this will impair the virus adsorption capacity of the finished filter.

Based on these data, a compromise with respect to the colloid dilution, sintering temperature, flowrate and specific surface area had to be met: The expense of both the latex and MS2 retention tests, and the procedural complexity of the latter, precluded performing a large number of these tests with a wide variety of elements modified using different parameters. Modifying the filters by dip-coating in a 1:1 dilution of as-delivered colloid with ultra-high purity water and sintering 1 h under reducing conditions at 550 °C yielded what was considered to the best balance of properties at acceptable process cost and complexity:

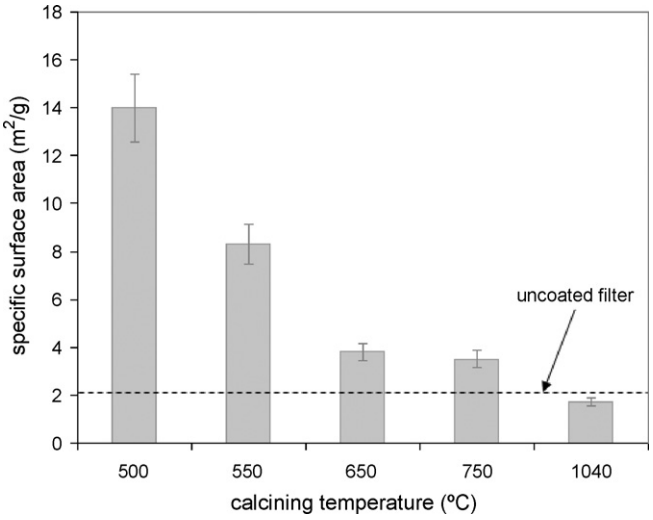

Fig. 8. Specific surface area as a function of calcining temperature of filter elements coated with $Y(OH)_x$-colloid diluted 1:1 with deionized water, calcined 1 h under flowing 92% N_2/8% H_2 and machined to remove the outer 2 mm of surface (refer to Fig. 2).

- considerable crystallinity in the Y_2O_3 coating (Fig. 2);
- an alkaline coating IEP which should promote the adsorption of negatively charged virus particles up to at least pH 9 (Figs. 3 and 4);
- a uniform distribution of the coating material across the filter wall (Fig. 7);
- a flowrate of 60 l/h at 3 bar/20 °C;
- a specific surface area of ≈8 m^2/g, which is approx. a factor of 4 greater than the SSA of the basic unmodified filter (Fig. 8).

All the data presented in the remainder of this paper pertains to filters prepared modified according to these parameters.

3.4. Retention performance

As noted in Section 2 above, initial retention tests were performed visually using dispersions of fluorescent yellow latex nanoparticles at pH 7. When such a bright yellow dispersion is pumped through the basic uncoated filter elements, the eluate exhibits a virtually unchanged coloration, indicating that little or no retention has taken place. This result is expected since (a) both the particles and the basic filter possess a negative zeta potential at pH 7 (refer to Ref. [17] [17] and Fig. 3, respectively) and therefore repel each other, and (b) the pores in the filter medium are at least one order of magnitude larger than the test particles and therefore no retention by the sieving effect can occur.

Filters coated with the 1:1 colloid dilution and calcined under a reducing atmosphere of 92% N_2/8% H_2 effectively remove the latex particles from the feed suspension at pH 7, as indicated by the complete absence of yellow coloration in the eluate. In this case the filter surface is largely positively charged (refer to Fig. 4), and consequently the negatively charged latex particles

[g] In the case of filters coated using the as-delivered colloid, an increase in flowrate could also be achieved by increasing the sintering temperature: as the calcining temperature is increased, the nanoparticles grow, and as this occurs, the number of pore channels is reduced and these grow in size. This results in a reduction of the capillary forces and consequently a decrease in the resistance to flow. However, as explained in relation to Fig. 8, the specific surface area and hence the filter capacity, is reduced.

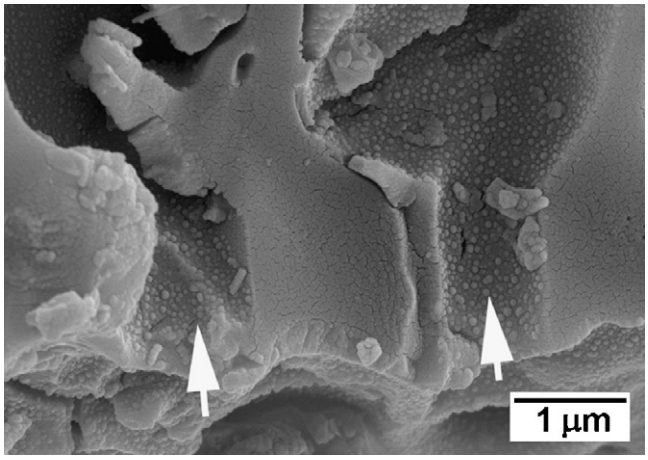

Fig. 9. SEM micrograph of the fracture surface of $Y(OH)_x$-coated filter medium (1:1 dilution) calcined at 550 °C under reducing conditions and subsequently challenged with an aqueous dispersion of negatively charged 50 nm latex particles at pH 7. Tightly packed arrays of latex particles are visible in the broken open pore channels of the kieselguhr (white arrows). The crazed surfaces adjacent to the channels are kieselguhr fracture surfaces covered with a relatively thick layer of sputtered Au–Pd. The filter was dried in air at 80 °C prior to SEM sample preparation.

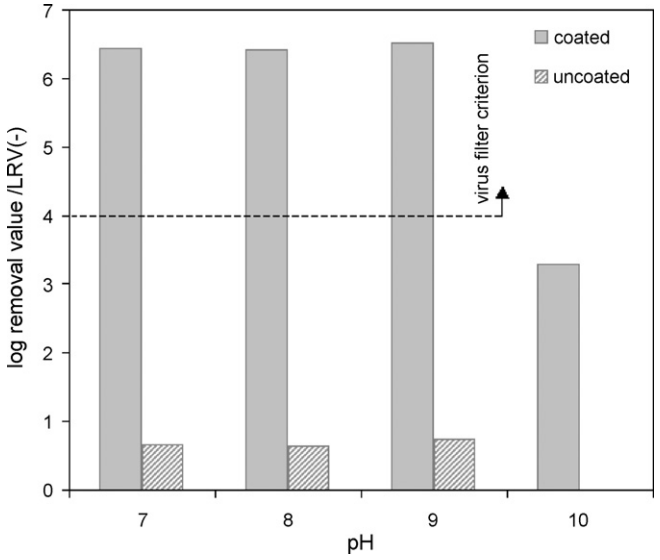

Fig. 10. Initial MS2 retention (first 500 ml) as a function of pH performed with freshly prepared colloid-coated elements (1:1 dilution of base colloid with water) calcined at 550 °C for 1 h under 92% N_2/8% H_2. The results for uncoated elements are shown for comparison. The feed water used was deionized water with NaCl added (400 µS/cm, 3 bar).

are attracted to it. That adsorption of individual particles on the filter surface, and not a sieving mechanism, is responsible for the removal of the particles from the water was confirmed by the subsequent SEM analysis of dried filter elements, as shown in Fig. 9. The analysis revealed myriad pore channels coated with latex particles, and while the channel diameters were obviously reduced by the adsorbed layer(s) of particles, no pores were detected which were completely blocked. No evidence for the agglomeration of latex particles and the subsequent sieving of agglomerates could be found.

After the tests with biologically inert nanoparticles proved successful, the microbiological tests with MS2 bacteriophages were commenced with. Fig. 10 shows that fresh-modified elements retain MS2 phages effectively up to and including pH 9 during at least the first 500 ml of model fluid (deionized + NaCl) water pumped through them. As expected from the zeta potential data above (Fig. 3), which shows the IEP of the calcined reduced yttria to be just under pH 10, the retention at pH 10 is significantly reduced. The fact that retention at a pH higher than the coating IEP is still better than that achieved with uncoated filters indicates that other mechanisms (van der Waals forces) also promote adsorption, and/or that viruses are also being filtered by mechanisms other than adsorption.

In more realistic tests modeling the application of the filters in a domestic environment, i.e. between the mains water supply and the tap of the kitchen sink, large amounts of potable tap water laced with a realistic concentration of MS2 (10^7 PFU/l) were pumped through fresh Y_2O_3-modified filters. As can be seen in Fig. 11, the filters effectively remove the bacteriophages from approx. 500 l of water before their adsorption capacity is exhausted and the 4 LRV lower retention limit stipulated by the USEPA is reached.

While these results are promising, a problem with filters operating on the adsorption principle is the occurrence of competitive adsorption of other species. Surface waters characteristically contain a certain concentration of HA which stem from the decomposition of organic materials (plant decay matter), and these are know to (a) cause physical fouling of finely porous filter media, and (b) possess surface charge characteristics similar to those of virus particles. The latter point is critical here, as this means that competitive adsorption will occur, depleting the filter of adsorption sites and reducing its capacity for virus adsorption. This is shown in Fig. 11, where in the presence of

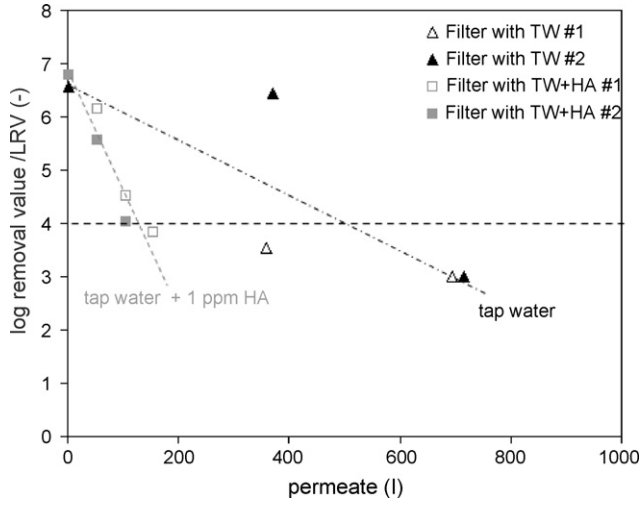

Fig. 11. Long-term MS2 retention test conducted with tap water (3 bar, pH 7.5) using two pairs of the coated filter elements (coating as in Fig. 8). For one pair water was used for the MS2 feed as obtained from the tap, for the second pair 1 ppm HA was added to the feed. Within each pair, the tests were conducted simultaneously using the same batch of feed water. As such, the wide scatter between the two HA-free data points at ≈360 l and their subsequent good agreement at ≈700 l cannot be explained. Unfortunately the complexity of the procedures and the limited availability of materials prevented more trials being performed.

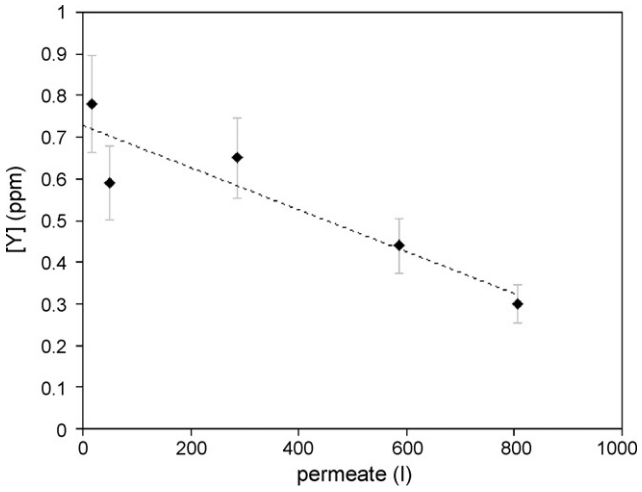

Fig. 12. Mass loss (with respect to the coating mass) due to the coating being washed out of modified filter elements (1:1 dilution of colloid with deionized water), as a function calcining temperature (1 h under 92% N_2/8% H_2). These tests were performed at 3 bar constant pressure with tap water.

1 ppm humic acid, the 4 LRV limit is reached after significantly less water has been pumped through the coated element compared to the amount filtered when the water is free of humic acid. Thus, while the filters function well in the HA-free case of high-quality potable water, slight contamination with HA and other negatively charged matter due to failures in, or insufficient standards of, water treatment will significantly impair their virus retention capability.

3.5. Coating integrity

The coatings of the filters used to perform the retention tests above were slowly washed out by the passage of water, as witnessed by the results of a chemical analysis by ICP which showed yttrium to be present in the eluate (Fig. 12). This effect had been encountered in the previous study involving $Zr(OH)_x$ nanoparticle coatings, however in that case the problem was much more severe.[17] The source of the problem is considered to be twofold: (1) as Fig. 1 shows, Y_2O_3 can be clearly identified as the crystalline phase developing at calcining temperatures around 500 °C, yet the broad diffraction peaks indicate that the long-range order of this phase is not yet fully developed. It may therefore be possible that there are water-soluble yttria precursors in the coating which are washed out during use; (2) the coating can be visualized as a closely packed array of nanoparticles, and if this particle array is to withstand the forces imposed by the flow of water through the microstructure, the particles must be firmly sintered to their nearest neighbors and to the underlying diatomaceous earth structure. Considering that the sintering onset temperatures of Y_2O_3 and SiO_2 can be estimated to be on the order of 1600 and 1070 °C, respectively,[h] considerable sintering will not have occurred in the filters calcined at 550 °C, and thus the coating will be relatively weakly bonded within themselves and to the underlying DE-based substrate.

Coinciding with the estimated sintering temperature of the basic SiO_2 filter, trials with elements calcined at higher temperatures showed that the washing-out phenomenon ceased to be a problem at 1040 °C. This result is, however, not without its drawbacks: The specific surface area of the filters drops dramatically (refer to Fig. 8), which is expected to cause a severe reduction in the retention capacity because the adsorber surface area is reduced. MS2 tests confirmed that retention was severely impaired in filters calcined at this high temperature, though it is unclear whether this is due only to the loss in capacity, or if a shift in the coating IEP also occurs.

4. Summary and conclusion

The aim of the presented work was to develop a high-flowrate ceramic water filter for point-of-use applications, which is capable of removing viruses from potable water. The targets for the filter were a flowrate of 60 l/h at less than 3 bar operating pressure and the microbiological boundary conditions stipulated by the USEPA for certifying virus filters, namely at least 99.99% retention (4 LRV) of virus particles 25 nm in diameter between pH 5 and 9 at a feed concentration of 10^7 PFU/l.

The basis for the development was diatomaceous earth-based ceramic filter elements of tubular geometry designed to remove dirt and bacteria from water by the sieving mechanism. DE possesses a negative surface charge in the specified pH range (IEP<2) and as such will repel water-borne viruses which generally exhibit a negative surface charge between pH 5 and 9. By applying a nanostructured Y_2O_3 coating to these filters using normal ceramic processing procedures (dip-coating, drying, sintering under reducing conditions), the internal surfaces of the filter take on a positive surface charge up to the IEP of the coating between pH 9 and 10. The charge difference between the filter surface and the virus particles leads to the effective adsorption of the latter: 5–6 LRV with respect to MS2 bacteriophages at 60 l/h with an operating pressure of 3 bar in the pH range 5–9.

These results are very promising and warrant further development of the idea and the process. Two immediate problems remain with the current state-of-the-art, specifically (1) a limited virus capacity/lifetime of the filters, and (2) washing out of the coatings during operation, and work is continuing to solve these problems. The inactivation of adsorbed viruses, the desorption of viruses from the filters, the regeneration of filters by the application of heat and other means, and the health effects of yttrium (oxide) on humans are also subjects of continuing investigations.

Acknowledgments

This work was supported by the Swiss Federal Office for Professional Education and Technology (CTI/KTI No. 7093.1). Thanks are extended to the following individuals for their contributions to this work: Mrs. N. Rittiner (Katadyn Products Inc.), Ms. D. Kinzer and Mr. S. Egli (Empa Laboratory 123), Mr. B. Sinnet (EAWAG), Prof. Dr. J. Fritsch (University of Applied

[h] Melting temperatures: $Y_2O_3 = 2410$ °C, $SiO_2 \approx 1600$ °C; rule of thumb: $T_{sintering} = 2/3 \times T_{melting}$.

Sciences, Ravensburg, Weingarten) and Mrs. R. Kohl and Mr. T. Luxbacher (Anton Paar).

References

1. Leong, L., Removal and inactivation of viruses by treatment processes for potable water and wastewater—a review. *Water Sci. Technol.*, 1983, **15**, 91–114.
2. Madaeni, S., The application of membrane technology for water disinfection. *Water Res.*, 1998, **33**, 301–308.
3. Clasen, T. and Menon, S., Microbiological performance of common water treatment devices for household use in India. *Int. J. Environ. Health Res.*, 2007, **17**, 83–93.
4. Gerba, C., Applied and theoretical aspects of virus adsorption to surfaces. *Adv. Appl. Microbiol.*, 1984, **30**, 133–168.
5. Brown, T., Malina Jr., J. and Moore, B., Virus removal by diatomaceous earth filtration—part 1. *J. Am. Water Works Assoc.*, 1974, **66**, 98–102.
6. Brown, T., Malina Jr., J. and Moore, B., Virus removal by diatomaceous earth filtration—part 2. *J. Am. Water Works Assoc.*, 1974, **66**, 735–738.
7. Chaudhuri, M., Amirhor, P. and Engelbrecht, R., Virus removal by diatomaceous earth filtration. *J. Environ. Eng. Div.: ASCE*, 1974, 937–953, NEE4.
8. Farrah, S., Preston, D., Toranzos, G., Girard, M., Erdos, G. and Vasuhdivan, V., Use of modified diatomaceous earth for removal and recovery of viruses in water. *Appl. Environ. Microbiol.*, 1991, **57**, 2502–2506.
9. Toranzos, G., Erdos, G. and Farrah, S., Virus adsorption to microporous filters modified by in situ precipitation of metallic salts. *Water Sci. Technol.*, 1986, **18**, 141–148.
10. Kattamuri, N., Shin, J., Kang, B., Lee, C., Lee, J. and Sung, C., Development and surface characterization of positively charged filters. *J. Mater. Sci.*, 2005, **40**, 4531–4539.
11. Lukasik, J., Cheng, Y.-F., Lu, F., Tamplin, M. and Farrah, S., Removal of microorganisms from water by columns containing sand coated with ferric and aluminum hydroxides. *Water Res.*, 1999, **33**, 769–777.
12. Lau, B., Harrington, G., Anderson, M. and Tejedor, I., Removal of nano and microparticles by granular filter media coated with nanoporous aluminium oxide. *Water Sci. Technol.*, 2004, **50**, 223–228.
13. Lee, J.-K., Liu, B., Rubow, K. and Zahka, J., Surface charge effects in particulate retention by microporous membrane filters in liquid filtration. In *Proceedings of the Institute of Environmental Sciences, vol. 1*, 1993, pp. 209–217.
14. Sobsey, M. and Jones, B., Concentration of poliovirus from tap water using positively charged microporous filters. *Appl. Environ. Microbiol.*, 1979, **37**, 588–595.
15. Oulman, C. and Baumann, E., Streaming potential in diatomite filtration in water. *J. Am. Water Works Assoc.*, 1964, **56**, 915–930.
16. Verwey, E. and Overbeek, J., *Theory of the Stability of Lyophobic Colloids—The Interaction of Sol Particles having an Electric Double Layer*. Elsevier, Amsterdam, 1948, pp. 46–50.
17. Wegmann, M., Michen, B., Luxbacher, T., Fritsch, J. and Graule, T., Modification of ceramic microfilters with colloidal zirconia to promote the adsorption of viruses from water. *Water Res.*, 2008, **42**, 1726–1734.
18. Graule, T., Wegmann, Michen, B., Clemens, F. and Ammann, B., Mikroporöses Filtermaterial, insbesondere zur Virenentfernung (Microporous filter material primarily for the purpose of virus removal, in German). Swiss patent application P 101391CH00, November 30, 2006.
19. Matthews, R., Classification and nomenclature of viruses; fourth report of the International Committee on Taxonomy of Viruses. *Intervirologie*, 1982, **17**, 1–80.
20. Zerda, K., Adsorption of viruses to charged-modified silica. Ph.D. Thesis. Baylor College of Medicine, Houston, TX, 1982.
21. Meschke, J. and Sobsey, M., Comparative reduction of Norwalk virus, poliovirus type 1, F+RNA coliphage MS2 and *Escherichia* in miniature soil columns. *Water Sci. Technol.*, 2003, **47**, 85–90.
22. Parks, G., The isoelectric points of solid oxides, solid hydroxides and aqueous hydroxo complex systems. *Chem. Rev.*, 1965, **65**, 177–198.
23. Shannon, R., Revised effective ionic radii and systematic studies of interatomic distances in halides and chalcogenides. *Acta Crystallogr.*, 1976, **A32**, 751–767.
24. Kosmulski, M., *Chemical Properties of Material Surfaces*. Marcel Dekker Inc., New York, 2001, pp. 165–170.
25. *Guide Standard and Protocol for Testing Microbiological Water Purifiers*. United States Environmental Protection Agency (USEPA), Washington, DC, 1987.
26. *Swiss Foodstuffs Book (Schweizerisches Lebensmittelbuch)*. Swiss Federal Office of Public Health (Bundesamt für Gesundheit, BAG), Bern, 2005, in German.
27. Fairbrother, F. and Mastin, H., Studies in electro-endosmosis. *J. Chem. Soc.*, 1924, **75**, 2319–2330.
28. Grabow, W. and Coubrough, P., Practical direct plaque assay for coliphages in 100-ml samples of drinking water. *Appl. Environ. Microbiol.*, 1986, **52**, 430–433.
29. Graule, T., Baader, F. and Gauckler, L., Casting uniform ceramics with direct coagulation. *Chemtech*, 1995, **25**, 31–37.